3

ELECTRONIC AND THERMAL PROPERTIES OF CARBON FIBERS

J.-P. Issi

1 Introduction

Despite the great deal of attention that carbon nanotubes (CN), the "ultimate" carbon fibers, is attracting because of their fascinating scientific aspects, the physical properties of the macroscopic version of carbon fibers remain a topic of great interest. Transport properties are no exception, since the various structures of carbon fibers and their particular geometry, have lead to interesting observations, which could not be made on bulk carbons and graphites. To this should be added the practical aspects since carbon fibers find unique applications, particularly in the form of composites. Also, as is the case for the bulk material, some carbon fibers may be intercalated with various species leading to a significant modification of their physical properties.

Because of their large length to cross section ratio, DC electrical resistivity measurements are relatively easy to perform on fibrous materials, in contrast to the case of bulk graphites (see Section 2). This allowed to separate the electronic and lattice contributions to the thermal conductivity using the Wiedemann–Franz law (Section 4). It also made possible high resolution electrical resistivity measurements leading to the discovery of quantum transport effects on intercalated (Piraux *et al*., 1985) and pristine fibers (Bayot *et al*., 1989). Also carbon fiber-based composites exploit their unique mechanical and thermal properties for which they find applications as light mechanical systems and heat transfer devices.

Transport properties have been reported for all varieties of carbon fibers including single wall (SWNT) and multiwall (MWNT) carbon nanotubes. Among macroscopic fibers, vapor grown carbon fibers (VGCF) are the most adequate for basic studies. They have the highest structural perfection when heat treated at high temperature. In that case, their transport properties are much like those observed for highly oriented pyrolytic graphite (HOPG). They display the highest electrical and thermal conductivities with respect to other carbon fibers. Also, they may be intercalated with donor and acceptor species which results in higher electrical conductivities, as is the case for HOPG. Similarly, their thermal conductivity and thermoelectric power are notably modified by intercalation.

The transport properties of carbon fibers are governed by the in-plane coherence length which mainly depends on the heat treatment temperature (cfr. e.g. Dresselhaus *et al*., 1988; Issi and Nysten, 1998). Some commercial pitch-derived carbon fibers (PDF) heat treated at high temperature have low electrical resistivities and thermal conductivities close to 1,000 $Wm^{-1}K^{-1}$, which largely exceeds that of copper. These high thermal conductivities associated to the fact that they may be obtained in a continuous form make them the ideal candidates for thermal management applications (Allen and Issi, 1985).

PAN-based fibers (PAN) are also continuous fibers, but they are generally disordered and their conductivity levels are rather low. One exception is the Celanese GY70, which exhibits a room temperature thermal conductivity of almost 200 $Wm^{-1}K^{-1}$ when it is heat treated at very high temperature (Nysten *et al*., 1987).

Some carbon nanotubes may have electrical conductivities comparable to VGCF heat treated at high temperature (Issi and Charlier, 1999). The thermal conductivity has not been measured on a single CN, but one may expect for such materials very high values associated to their unique mechanical properties.

VGCF's heat treated at high temperature are semimetallic with very few charge carriers as compared to metals. Also, like HOPG, they have generally more than one type of charge carriers, which complicates the analysis of electronic transport properties data. Owing to the small density of charge carriers, associated with a relatively large lattice in-plane thermal conductivity, heat is almost exclusively carried by the lattice vibrations above the liquid helium temperature range.

Because of the favorable length to cross section ratios (Chieu *et al*., 1982; Issi, 1992), four-probe electrical DC measurements may be readily performed on intercalated fibers contrary to the case of the bulk material. High resolution electrical resistivity measurements have thus been performed on graphite fibers allowing the investigation of weak localization effects and the separation of the ideal resistivity from the residual resistivity in spite of their very low residual resistivity ratio (RRR) – the ratio of the resistance at 300 K to that at 4.2 K (Piraux *et al*., 1986a,b).

A few comprehensive reviews have been recently published on the transport properties of pristine and intercalated carbon fibers (Dresselhaus *et al*., 1988; Issi, 1992; Issi and Nysten, 1998). We shall refer to them when necessary for more detailed information.

In chapter 3, volume 1 of this series, to which we shall refer hereafter as I, we have discussed the basic aspects of the transport properties of carbons and graphites (Issi, 2000). We have pointed out in I that there were no qualitative differences between the basic transport phenomena in bulk and fibrous materials. So, we will mainly concentrate here on the specific aspects related to fibers which were not discussed in detail in I. These are essentially due to their geometry and their very small cross sections. We will also discuss in some detail the thermal conductivity of fibers, since it was not presented in I. We will refer, when necessary, to the basic concepts developed in I. Thus, in this chapter emphasis will be placed on:

- the thermal conductivity of pristine fibers;
- the effect of intercalation on the transport properties;
- the thermal and, to a lesser extent, the electrical conductivity of composites;
- the experimental difficulties associated to measurements on fibrous materials.

The chapter is organized as follows. First, we shall point out some experimental aspects specific to fibrous materials, including CNs (Section 2). Then we shall discuss the electrical conductivity (Section 3) the thermal conductivity (Section 4) and the thermoelectric power (Section 5) of various types of pristine carbon fibers. The effect of intercalation on these transport properties will be discussed in Section 6. Then, after briefly showing how transport measurements may be used to characterize carbon fibers (Section 7), we will consider the situation for carbon fiber composites (Section 8).

2 Experimental challenges

There are some specific problems associated to the measurement of the transport properties on fibrous materials which are not encountered in bulk materials. It is obvious that this should be the case for measurements on individual nanotubes where samples are of submicronic sizes and are quite difficult to handle. For other reasons (cfr. below), it also applies for the measurement of the thermal conductivity on carbon fibers.

For fibers with diameters around 10 μm, electrical resistivity, magnetoresistance, and thermoelectric power measurements do not generally present serious problems. The problems encountered in the case of *electrical resistivity* measurements are due to the nature of the samples. Indeed, the diameters of the fibers are not the same along a given filament and from one filament to another of the same batch. Also, the cross sections of the samples are not always cylindrical. This makes it difficult to calculate the conductivity (or resistivity) from the measured resistance. So, the determination of the fiber cross section introduces large uncertainties in the estimation of the absolute values of the resistivities or conductivities. Since electrical parameters such as electrical current and voltage, may be measured with great accuracy, the data obtained are more accurate with regard to temperature variation than with regard to absolute magnitudes. Fortunately, for the interpretation of the experimental results it is more important to know the temperature variation than the absolute values. These problems are not met in magnetoresistance and thermoelectric power measurements since the knowledge of the samples cross sections is not needed to calculate these transport coefficients.

More generally speaking, it is a rather easy task to measure the electrical resistivity, except for extreme cases of very low or very high values. However, the measurement of samples of submicronic sizes requires a miniaturization of the experimental system, which may in some instances attain a high degree of sophistication. This is particularly true for the case of single CNs, where one has to deal with samples of a few nm diameter and about a μm length (Issi and Charlier, 1999). One has first to detect the sample, then apply to it electrical contacts, which means, in a four-probe measurement, four metallic conductors, two for the injected current and two for measuring the resulting voltage. This requires the use of nanolithographic techniques (Langer *et al*., 1994). Besides, one has to characterize the CN sample which electrical resistivity is measured in order to determine its diameter and helicity, which leads to the knowledge of the electronic structure.

Thermal conductivity is a very delicate measurement to perform on a single fiber and prohibitively difficult on a single CN. This explains why little attention had been paid to the thermal conductivity of carbon fibers until the beginning of the 1980s and while still no data are available on single CNs. More generally, thermal conductivity measurements are time consuming and very delicate to perform. This is particularily true for samples of small cross-sections, as it is the case for carbon fibers (Piraux *et al*., 1987). Indeed, since the fibers are usually of small diameters ($\sim 10^{-5}$ m) it is difficult to make sure that the heat losses in the measuring system do not by far exceed the thermal conductance of the samples measured. The thermal conductance is defined as the heat flow through the sample per unit temperature difference. One may measure a bundle of fibers to increase the thermal conductance with respect to heat losses, but it is not always possible to realize samples in the form of bundles. Moreover, in order to be able to get an insight into the mechanisms of the thermal conductivity of these fibers, it is necessary to measure the temperature variation of this property over a wide temperature range on a single well characterized fiber, as was done for VGCFs (Piraux *et al*., 1984).

In order to measure the temperature variation of the thermal conductivity of a single VGCF or a small bundle of continuous fibers one should use a sample holder specially designed to reduce significantly heat losses. This sample holder, which was designed for measuring samples with very small thermal conductances, is described in detail elsewhere (Piraux *et al*., 1987). It is based on the principle of a thermal potentiometer, adapted to measure the thermal conductivity of brittle samples of very small cross-sections and low thermal conductances (10^{-6}–$10^{-2}\,\mathrm{WK}^{-1}$) over a wide temperature range.

In some cases the fibrous geometry presents some advantages with respect to bulk carbons and graphites. In lamellar structures like that of graphites the electrical conductivity is highly anisotropic. This anisotropy is even higher in their acceptor intercalation compounds where it may exceed 10^6. In that case measuring the in-plane DC electrical resistivity on bulk samples presents a real problem, since one needs a sample of extremely large length to cross section ratio to insure that the electrical current lines be parallel. Fibers have very high length to cross section ratios and thus electrical resistivity measurements could easily be realized on them.

3 Electrical resistivity

We have introduced in I what we believe are the most important features pertaining to the electrical resistivity of carbons and graphites. We have insisted on the effect of the semimetallic band structure on the electronic behavior in general, and, more particularly, on electron scattering mechanisms in these materials. This applies also for VGCFs heat treated at high temperatures and to some CNs. We have also discussed in some length the effect of weak localization. Incidentally, the particular geometry and the defect structure of carbon fibers have allowed the observation of these *quantum transport effects* for the first time in carbons and graphites (Piraux *et al*., 1985).

We have seen that the Boltzmann electrical conductivity for a given group of charge carriers is proportional to the charge carrier density and mobility. Concerning the scattering mechanisms, the main contributions to the electrical resistivity of metals, ρ, consists of an intrinsic temperature-sensitive ideal term, ρ_i, which is mainly due to electron–phonon interactions and an extrinsic temperature independent residual term, ρ_r, due to static lattice defects.

As is the case for any solid, the temperature dependence of the electrical resistivity of various classes of carbon-based materials is very sensitive to their lattice perfection. The higher the structural perfection, the lower the resistivity. Samples of high structural perfection exhibit room temperature resistivities below $10^{-4}\Omega\,\mathrm{cm}$, while partially carbonized samples exhibit resistivities higher than $10^{-2}\Omega\,\mathrm{cm}$ which generally increase with decreasing temperature. An intermediate behavior between these two extremes is represented by curves which depend less on the heat treatment temperature (HTT) and does not show significant temperature variations (cfr. I).

The first comprehensive measurements of the temperature dependence of the electrical resistivity of pitch-based carbon fibers were performed by Bright and Singer (1979). They investigated radial as well as random samples heat treated at various temperatures ranging from 1,000 to 3,000 °C. They have shown that the magnitude of the resistivity, as well as its temperature variation, depends on the heat treatment temperature. The same kind of observations were made for VGCFs.

In I we have presented the temperature dependence of the electrical resistivity of many carbon materials, including fibers. As an additional illustrative example we show in Fig. 3.1

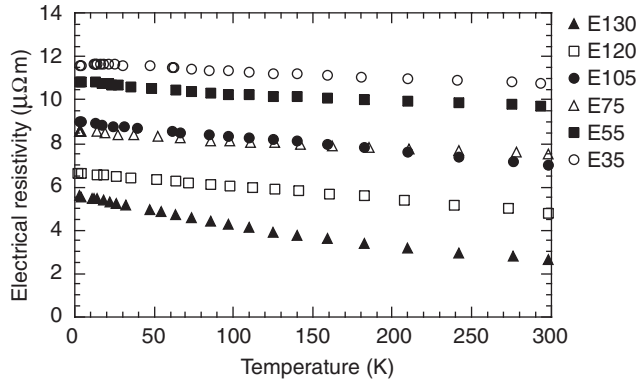

Figure 3.1 Temperature dependence, from 2 to 300 K, of the zero-field electrical resistivity of six samples of pitch-based carbon fibers heat treated at various temperatures (Nysten *et al*., 1991a).

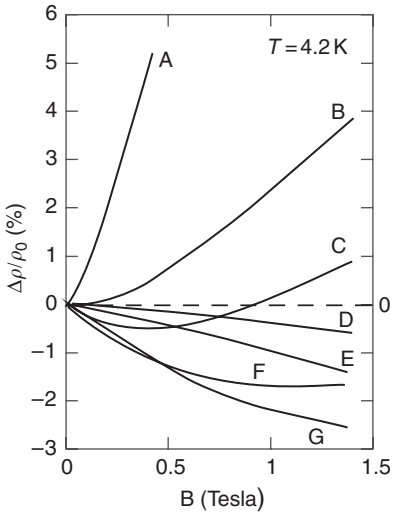

Figure 3.2 Transverse magnetoresistance for ex-mesophase pitch carbon fibers heat treated at different temperatures ranging from 1,700 (sample D) to 3,000 °C (samples ABCF). Samples A, B, C, and F, which were heat treated at the same temperature, exhibit different residual resistivities (measured at 4.2 K): 3.8, 5.1, 7.0, and $6.6 \times 10^{-4}\,\Omega\,\text{cm}$ respectively. Samples G and E were heat treated at 2,500 and 2,000 °C, respectively (from Bright, 1979).

how this temperature dependence may vary with the heat treatment temperature, i.e. with crystalline perfection. In this figure the temperature dependence of the electrical resistivity of six samples of pitch-based carbon fibers heat treated at various temperatures are compared (Nysten *et al*., 1991a). Except for the E35 fibers, the resistivies of all the samples investigated decrease with increasing temperature. This dependence was also observed on

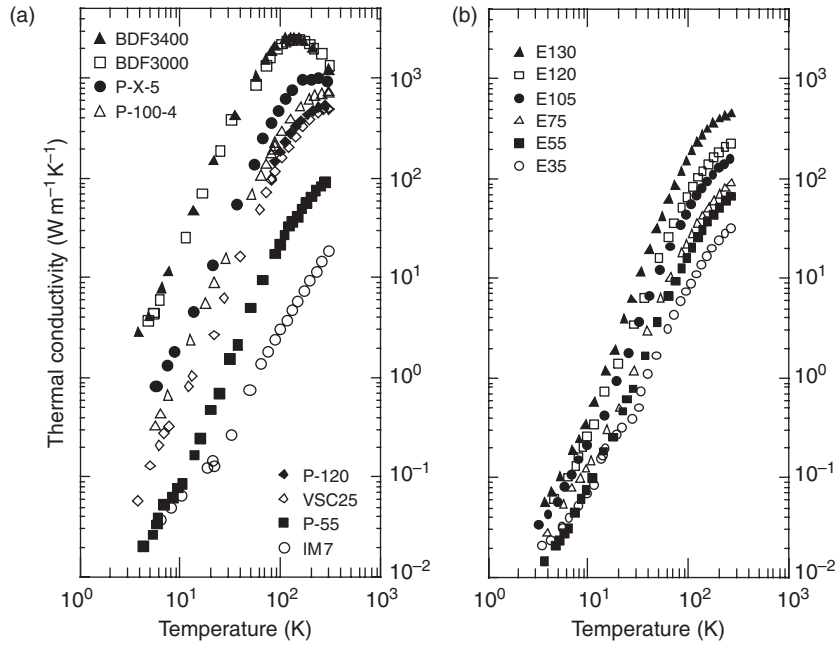

Figure 3.3 (a) Comparison of the temperature variation of the thermal conductivity of pristine carbon fibers of various origins. Since scattering below room temperature is mainly on the crystallite boundaries, the phonon mean free path at low temperatures, i.e. below the maximum of the thermal conductivity versus temperature curve is temperature insensitive and mainly determined by the crystallite size. The largest the crystallites the highest the thermal conductivity. Note that some VGCF and PDF of good crystalline perfection show a dielectric maximum below room temperature. For decreasing lattice perfection the maximum is shifted to higher temperatures (Issi and Nysten, 1998); (b) Temperature dependence of the thermal conductivity of the six samples of pitch-based carbon fibers heat treated at various temperatures, the same fibers with electrical resistivity is presented in Fig. 3.1 (Nysten *et al*., 1991b).

other carbon fibers (Bayot *et al*., 1989) and pyrocarbons (cfr. I, Figs 3.3 and 3.4). Such a behavior was explained in the frame of the weak localization theory (Bayot *et al*., 1989).

As explained in I, weak localization generates an additional contribution to the low temperature electrical resistivity which adds to the classical Boltzmann resistivity. Indeed, in the weak disorder limit, which is also the condition for transport in the Boltzmann approximation, i.e. when $k_F.l \gg 1$, where k_F is the Fermi wave vector and l the mean free path of the charge carriers, a correction term, $\delta\sigma^{2D}$, is added to the Boltzmann classical electrical conductivity, $\sigma^{2D}{}_{Boltz.}$:

$$\sigma^{2D} = \sigma^{2D}{}_{Boltz.} + \delta\sigma^{2D} \tag{1}$$

The additional term $\delta\sigma^{2D}$ accounts for localization and interaction effects which both predict a similar temperature variation (cfr. I).

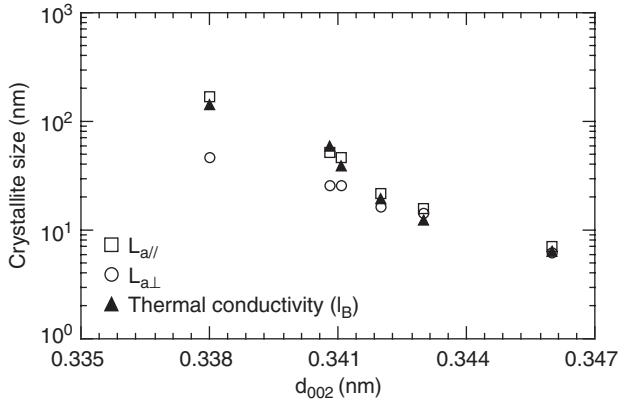

Figure 3.4 Dependence on the interlayer spacing d_{002} of the in-plane coherence lengths and the phonon mean free path for boundary scattering, l_B (Nysten *et al*., 1991b).

A magnetic field destroys this extra contribution (Bayot *et al*., 1989) and restores the classical temperature variation predicted by the standard two band model (Klein, 1964). This results in an apparent negative magnetoresistance.

We have briefly discussed in I the positive and negative magnetoresistances in carbons and graphites and the interpretation of the latter in terms of weak localization effects. The positive magnetoresistance at low magnetic fields depends essentially on the carrier mobilities. The *negative magnetoresistances*, which was first observed in pregraphitic carbons by Mrozowski and Chaberski (1956) and later on in other forms of carbons, is a decrease in resistivity with increasing magnetic field. This effect was also observed in PAN-based fibers (Robson *et al*., 1972, 1973), pitch-derived fibers (Bright and Singer, 1979), and vapor-grown fibers (Endo *et al*., 1982) and was interpreted later on in the frame of the weak localization theory for two dimensional systems (Bayot *et al*., 1989).

We present in Fig. 3.2 the results obtained by Bright (1979) for the transverse magnetoresistance at 4.2 K for ex-mesophase pitch carbon fibers heat treated at different temperatures ranging from 1700 °C (sample D) to 3,000 °C (samples A, B, C, and F). It is worth noting that the four samples A, B, C, and F were all heat treated at the same temperature, but exhibited different residual resistivities (measured at 4.2 K); 3.8, 5.1, 7.0, and 6.6, $10^{-4}\Omega$ cm respectively. Higher residual resistivities correspond to higher disorder. Samples G and E were heat treated at 2,500 and 2,000 °C respectively.

It should be also noted that highly graphitized fibers, i.e. those heat treated at the highest temperatures, present large positive magnetoresistances, as expected from high mobility charge carriers. This explains why samples A and B which exhibit the lowest residual resistivities exhibit also large positive magnetoresistances, even at low magnetic fields. With increasing disorder, a negative magnetoresistance appears at low temperature, where the magnitude and the temperature range at which it shows up increase as the relative fraction of turbostratic planes increases in the material (Nysten *et al*., 1991a).

The results obtained, which are presented in Fig. 3.2, were later confirmed by Bayot *et al*. (1989) and Nysten *et al*. (1991a), who found the same qualitative behavior on different samples of pitch-derived carbon fibers.

4 Thermal conductivity

4.1 Electron and phonon conduction

Around and below room temperature, heat conduction in solids is generated either by the charge carriers as is the case for pure metals or by the lattice waves, the phonons, which is the case for electrical insulators. In carbons and graphites, owing to the small densities of charge carriers, associated with a relatively large in-plane lattice thermal conductivity due to the strong covalent bonds, heat is almost exclusively carried by the phonons, except at very low temperatures, where both contributions may be observed. In that case, the total thermal conductivity is expressed:

$$\kappa = \kappa_E + \kappa_L \tag{2}$$

where κ_E is the electronic thermal conductivity due to the charge carriers and κ_L is the lattice thermal conductivity due to the phonons.

We will show in Section 6.6 that, because of their large length to cross section ratio, it is possible to separate κ_E and κ_L in carbon fibers, when they contribute by comparable amounts as it is the case at low temperature for pristine fibers and at various temperatures for the intercalated material.

In Fig. 3.3a we present the temperature variation of the thermal conductivity of pristine carbon fibers of various origins and precursors. In Fig. 3.3b we compare the temperature dependence of the thermal conductivity of the six samples of pitch-based carbon fibers heat treated at various temperatures (Nysten *et al*., 1991b). These are the same set of fibers which electrical resistivity is presented in Fig. 3.1.

4.2 Lattice conduction

It was shown that the lattice thermal conductivity of carbon fibers is directly related to the the in-plane coherence length (Nysten *et al*., 1991b; Issi and Nysten, 1998). Thus thermal conductivity measurements allow to determine this parameter. It also enables to compare between shear moduli (C_{44}) and provide information about point defects.

In Fig. 3.4, the dependence of the in-plane coherence lengths, L_a, and the phonon mean free paths for boundary scattering, l_B, on the interlayer spacing d_{002} is presented (Nysten *et al*., 1991b). One may see that the phonon mean free path for boundary scattering is almost equal to the in-plane coherence length as determined by x-ray diffraction, L_a. Thermal conductivity measurements may thus be used as a tool to determine this parameter, especially for high L_a values where x-rays are inadequate. One may also observe that the concentration of point defects such as impurities or vacancies, decreases with increasing graphitization.

A naive way to understand how lattice conduction takes place in crystalline materials, is by considering the case of graphite in-plane, assuming that it is a two-dimensional (2D) system, which is not too far from the real situation around room temperature. The atoms in such a system may be represented by a 2D array of balls and springs and any vibration at one end of the system will be transmitted via the springs to the other end. Since the carbon atoms have small masses and the interatomic covalent forces are strong, one should expect a good transmission of the vibrational motion in such a system and thus a good lattice thermal conductivity. Any perturbation in the regular arrangement of the atoms, such as defects or atomic vibrations, will cause a perturbation in the heat flow, thus giving rise to scattering which decreases the thermal conductivity.

In order to discuss the lattice thermal conductivity results of isotropic materials, one generally uses the Debye relation:

$$\kappa_g = \frac{1}{3} C\, v\, l \tag{3}$$

where C is the lattice specific heat per unit volume, v is an average phonon velocity, the velocity of sound, and l the mean free path which is directly related to the phonon relaxation time, τ, through the relation $l = v\,\tau$. For a given solid, since the specific heat and the phonon velocities are the same for different samples, the sample thermal conductivity at a given temperature is directly proportional to the phonon mean free path.

VGCF's heat treated at 3,000 °C, may present room temperature heat conductivities exceeding 1,000 $Wm^{-1}K^{-1}$ (Fig. 3.3a). The thermal conductivity of less ordered fibers may vary widely, about two orders of magnitude, according to their microstructure (Issi and Nysten, 1998). At low temperature, the lattice thermal conductivity is mainly limited by phonon-boundary scattering and is directly related to the in-plane coherence length, L_a.

When scattering is mainly on the crystallite boundaries, the phonon mean free path should be temperature insensitive. Since the velocity of sound is almost temperature insensitive, the temperature dependence of the thermal conductivity should follow that of the specific heat. Thus, the largest the crystallites the highest the thermal conductivity. Well above the maximum, phonon scattering is due to an intrinsic mechanism: phonon–phonon umklapp processes, and the thermal conductivity should thus be the same for different samples.

Around the thermal conductivity maximum, scattering of phonons by point defects (small scale defects) is the dominating process. The position and the magnitude of the thermal conductivity maximum will thus depend on the competition between the various scattering processes (boundary, point defect, phonon, …). So, for different samples of the same material the position and magnitude of the maximum will depend on the point defects and L_a, since phonon–phonon interactions are assumed to be the same. This explains why, by measuring the low temperature thermal conductivity, one may gather information about the in-plane coherence length L_a and point defects. This shows also that by adjusting the microstructure of carbon fibers, one may tailor their thermal conductivity to a desired value.

Some VGCF and PDF of good crystalline perfection show a maximum below room temperature and, with decreasing lattice perfection the maximum is shifted to higher temperatures (Issi and Nysten, 1998).

Recently, the thermal conductivities of ribbon-shaped carbon fibers produced at Clemson University and graphitized at 2,400 °C and those of commercial round fibers graphitized at temperatures above 3,000 °C were measured and the data were compared. It was shown that, in spite of the difference in the heat treatment temperature, the two sets of fibers presented almost the same electrical and thermal conductivities. This clearly shows that, for a given HTT, spinning conditions have an important influence on the transport properties of pitch-based carbon fibers. By modifying these conditions, one may enhance these conductivities, which is important for practical applications since HTT is a costly process (cfr. Part 1, § 2 of this issue).

Oddly enough, though the electrical and thermal conductivities of pristine carbon fibers are generated by different entities, charge carriers for the electrical conductivity and phonons for the thermal conductivity, a direct relation between the two parameters is observed at room temperature (Nysten *et al*., 1987). This is related to the fact that both transport properties depend dramatically on the structure of the fibers. They both increase

with the in-plane coherence length. As a practical result of the direct relation between these transport coefficients for fibers with the same precursor, once the electrical resistivity is measured one can determine the thermal conductivity.

5 Thermoelectric power

We have introduced in I the two mechanisms responsible for the thermoelectric power, a *diffusion and a phonon drag mechanism* and have given an expression for the diffusion thermoelectric power. From this expression, it was found that the diffusion thermoelectric power for a degenerate electron gas varies as the inverse of the Fermi energy, or carrier density. This explains why semimetals like graphites exhibit higher partial diffusion thermoelectric powers than metals or graphite intercalation compounds (GICs). We have also presented in I the temperature variation of the thermoelectric power of a graphite single crystal.

We present in Fig. 3.5 the temperature dependence of the thermoelectric power of six samples of pitch-based carbon fibers heat treated at various temperatures. The samples investigated are the same whose electrical resistivities are presented in Fig. 3.1 and thermal conductivities in Fig. 3.3b. In Fig. 3.6 the earlier results of Endo and co-workers (1977) on the temperature dependence of the thermoelectric power of vapor grown (benzene-derived) carbon fibers are shown. In this figure VGCFs heat treated at two different temperatures are compared to the as-grown material.

It may be seen from all these curves that, as is the case for the bulk material, the thermoelectric power of carbon fibers is very sensitive to lattice perfection. For as grown fibers or fibers heat treated at low temperatures, the thermoelectric power is low and does not vary significantly with temperature; the room temperature thermoelectric power may even be

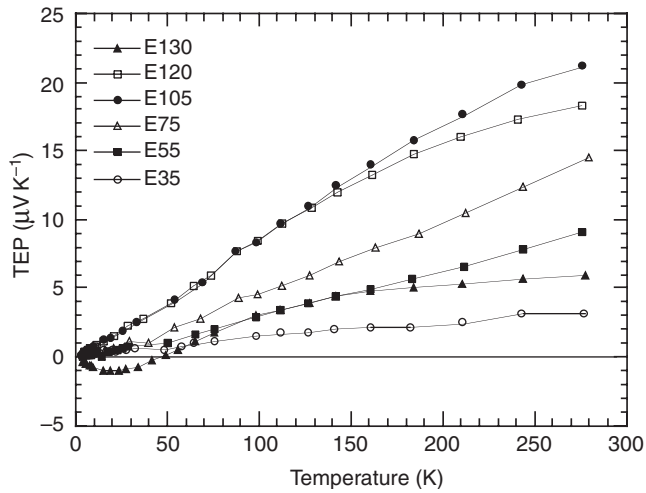

Figure 3.5 Temperature dependence of the thermoelectric power of six samples of pitch-based carbon fibers heat treated at various temperatures, the same fibers with electrical resistivity is presented in Fig. 3.1 and thermal conductivity in Fig. 3.3b (Issi and Nysten, 1998).

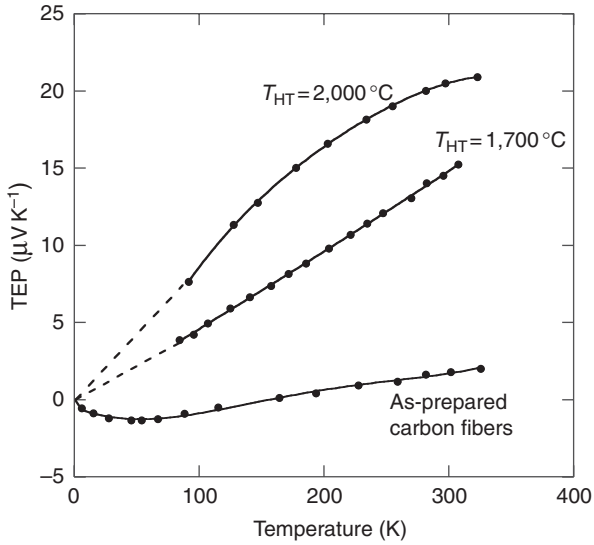

Figure 3.6 Temperature dependence of the thermoelectric power of three VGCFs heat treated at two different temperatures compared to the as-grown material (Endo *et al*., 1977).

negative. Fibers heat treated at higher temperature exhibit a marked temperature dependence and higher magnitudes for the thermoelectric power. Then, if the heat treatment temperature is further increased the thermoelectric power decreases.

This behavior should naturally be correlated to that of the in-plane coherence length, L_a, or the 2D cristallites sizes, In I we have presented the room temperature thermoelectric power of various experimental pitch-based carbon fibers versus in-plane coherence length, L_a (fig. 3.5b in I). It was shown that the thermoelectric power increases first rapidly with L_a, reaches a maximum, then decreases first rapidly then slowly with L_a. For L_a larger than 300 nm the thermoelectric power is positive around room temperature.

The temperature variation of the thermoelectric power of bundles of SWNTs has been measured from 4.2 to 300 K by Hone *et al*. (1998). They have also reported on the temperature dependence of the electrical resistivity of their samples in the same temperature range. Three samples were investigated, two pristine and one sintered. Their thermoelectric powers exhibited the same qualitative behavior and almost the same magnitudes (Fig. 3.7). They were found to be positive over all the temperature range investigated. They increase first linearly at low temperature, then tend to reach an almost constant value around 100 K, to increase slowly again with temperature around 200 K. The room temperature values, around 50 μVK^{-1}, are considerably higher than that of metallic samples (a few μVK^{-1}), but comparable to those observed in semimetals. Oddly enough, the temperature variation resembles more that observed in graphite intercalation compounds (Fig. 3.12) than in the pristine material, though the room temperature value measured in SWNTs is about twice that reported for GICs.

In general, the interpretation of thermoelectric power data in most materials is a delicate job and this is particularly true for the case of carbons and graphites. We have seen for example that the relation between the thermal conductivity or electrical conductivity versus in-plane coherence length is straightforward. We observe an enhancement of these properties

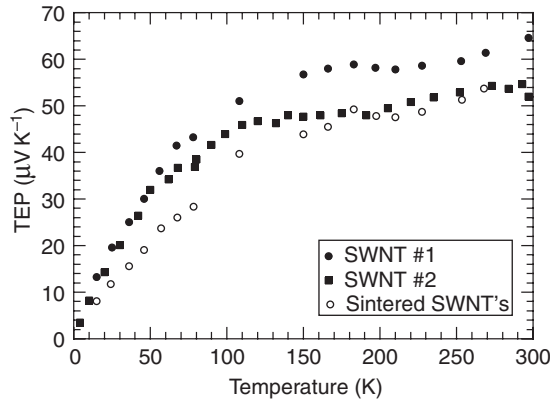

Figure 3.7 Temperature dependence of the thermoelectric power of three single wall carbon nanotube samples (Hone *et al*., 1998).

with increasing L_a. This is due to the fact that both the electron and phonon mean free paths increase with L_a, i.e. with crystalline perfection. For the thermoelectric power the situation is different. This is due to the fact that the thermoelectric power is much more sensitive to the carrier density than to the scattering mechanism. In addition, when electrons and holes contribute to conduction, they have opposite effects on the thermoelectic power since the latter is negative for electrons and positive for holes. So, unless one knows with some accuracy the band structure of the sample and the scattering mechanism, it is difficult to predict which contribution, electron or hole, will dominate the scene.

6 Fibrous intercalation compounds

6.1 Introduction

Since the early 1980s, a large amount of experimental data has been published on the temperature variation of the electrical resistivity of intercalated carbon fibers of various origins. Fewer results are available on the thermal conductivity of these compounds (Issi, 1992). This is due to the difficulties associated with thermal conductivity measurements on samples of small cross sections that we discussed in Section 2.

The *charge transfer* resulting from intercalation increases the carrier density, while defects due to the intercalation process reduces the electronic mobility, but generally in a smaller relative amount. The net result of intercalation is thus an increase in *electrical conductivity* (Fig. 3.8). Most types of fibers have been intercalated and some fibrous acceptor GIC were found to exhibit room temperature electrical conductivities comparable to that of the best metallic conductors. The situation is different for the *thermal conductivity* which, depending on the compound and the temperature range investigated, may increase or decrease after intercalation.

Acceptor GICs are highly anisotropic electronic systems and their charge carriers, originating from the charge transfer from the intercalate, form 2D hole gases. Their Fermi surfaces consists in circles for stage-1 compounds and in cylinders for higher stage compounds (Blinowsky *et al*., 1980). It is interesting to note that the same 2D model may be applied for

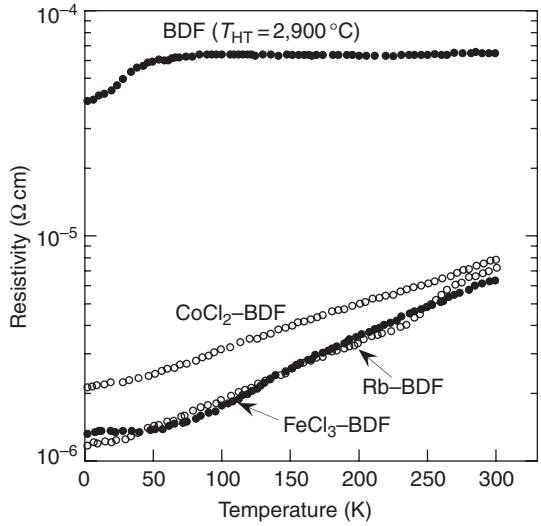

Figure 3.8 Effect of intercalation by a donor (Rb) and acceptor ($FeC1_3$) intercalate on the temperature variation of the electrical resistivity of a benzene-derived VGCF heat treated at 29,000 °C (Chieu *et al*., 1983).

all acceptor compounds and the value of the Fermi level, which is directly related to the magnitude of the charge transfer, determines the value of the ideal resistivity.

For *donor compounds*, since the anisotropy varies considerably with the intercalated species, and from one stage to another for a given intercalate, the situation is far more complicated. This is why, despite the considerable amount of theoretical work performed on the band structure of donor compounds, the situation is not as clear as it is for acceptor compounds. This has a direct bearing on our understanding of the transport properties of these compounds.

As a direct consequence of the anisotropic band structure, the *electrical resistivity* of acceptor GICs is also highly anisotropic. The ratio of the in-plane conductivity to that along the c-axis may reach six orders of magnitude at room temperature for some acceptor GICs (Dresselhaus and Dresselhaus, 1981).

Since it is dependent on the phonon spectrum, which is less anisotropic than the electron distribution, the *lattice thermal conductivity* is also less anisotropic than the electrical resistivity (Issi *et al*., 1983). The *thermoelectric power* presents a smaller anisotropy than that of the two other transport properties (Issi, 1992).

6.2 Electrical resistivity

As a typical example among others, we present in Fig. 3.8 the effect of intercalation on the temperature variation of the electrical resistivity of a VGCF heat treated at 2,900 °C (Chieu *et al*., 1983). We may see that there is a significant decrease in resistivity due to the intercalation of either donor (Rb) or acceptor ($FeCl_3$ and $CoCl_2$) intercalated species. The temperature variation of the intercalation compounds thus obtained exhibit metallic behaviors with a room temperature electrical resistivities 3–4 times that of pure copper.

The in-plane resistivity data in acceptor GICs is interpreted by considering the 2D hole gas in the graphene host layers, which is fully described once its Fermi energy is known. This 2D hole gas interacts with the phonons and defects which are present in the host layers generating a finite resistivity. In the presence of weak disorder hole–hole interaction may also take place at low temperature.

The *ideal electrical resistivity*, which is due to electron–phonon scattering, should vary as T^n with $n = 5$ at very low temperature. Then n should gradually decrease with increasing temperature until it reaches unity around and above the Debye temperature. The temperature dependence of the ideal resistance in GICs was found instead to fit the relation (see e.g. Dresselhaus and Dresselhaus, 1981):

$$R(T) = BT + CT^2 \tag{4}$$

where B and C are constants, which may vary according to the compound considered.

In acceptor GICs the *ideal electrical resistivity* depends on the carrier density, N, and on the phonon spectrum of the host material (Issi and Piraux, 1986), which determines the electron-phonon relaxation time. The amount of charge transfer generating N varies with the nature of the intercalate and with the stage of the compound. The phonon dispersion relations do not vary significantly from one compound to another. Thus, if the same 2D band model is assumed for all acceptor GICs, the differences in ideal resistivities for fibrous GICs samples should be entirely ascribed to different Fermi energies. For metal chlorides GICs, since their Fermi energies are almost the same for a given stage and do not vary significantly from one stage to the other for lower stages, the ideal resistivities are not expected to be much different from one compound to another (cfr. I).

We have discussed in I the electron–phonon interaction in pristine carbons and graphites and concluded that, contrary to 3D metals, the charge carriers interact with subthermal phonons except at very low temperatures. In the case of acceptor GICs the situation is intermediate between that of 3D metals and that of the pristine material. This means that electron–phonon interactions are weaker in GICs than in 3D metals at a given temperature, but stronger than in the pristine material (Issi and Nysten, 1998).

Measurements performed on various low stages fibrous acceptor GICs confirmed the validity of relation (4). An almost linear variation of the ideal resistivity at low temperature and an almost T^2 behavior around room temperature was observed. Oddly enough, contrary to what is generally predicted and observed, a higher power law is found at higher temperature. This is difficult to ascribe to an electron–phonon scattering mechanism all over the temperature range. Instead, in the presence of weak disorder, the relaxation time for 2D hole–hole interactions should vary linearly at low temperatures. Thus, it is reasonable to ascribe the low temperature linear dependence to strong hole–hole interactions.

The *residual resistivity* of acceptor GICs, is due to hole-defect scattering. The defects are those which were initially in the pristine host material to which are added those introduced during the intercalation process. Scattering from the defects of both origins will combine in the temperature region where the mean free paths associated to the two scattering processes are comparable in magnitude. The residual resistivity will then depend on the host material and on the intercalated species. In pristine fibers the defect structure varies widely according to the type of fiber, heat treatment temperature and quality of the precursor for a given type of fiber. Thus, since carbon fibers provide a large variety of host defect structures in GICs,

fibrous acceptor GICs are ideal candidates to investigate 2D weak localization and interaction effects (Issi, 1992).

First, acceptor GICs are natural 2D electronic systems, since the 2D behavior results from the distribution of the charge carriers, which are strongly localized in the graphene planes and which may be considered as quasi free carriers – though weakly localized – only for motion along these planes. This leads to the 2D electronic band structure. Second, the possibility of varying the defect structure of the host material over wide ranges in acceptor GICs allows large experimental possibilities for investigating the phenomena of weak localization and electron–electron interactions. Finally, the Fermi level may be modified by varying the nature of the intercalate and its concentration.

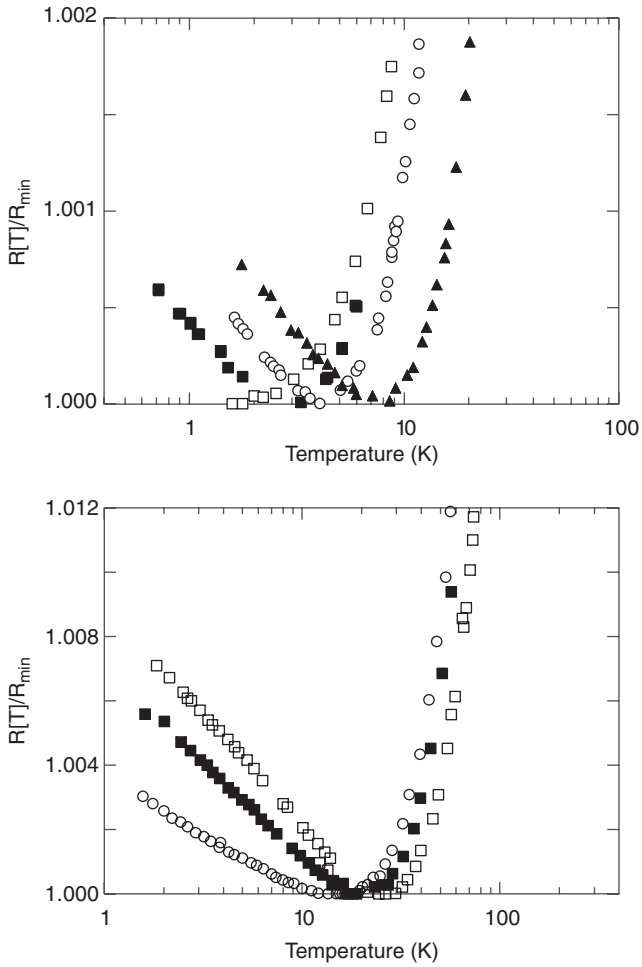

Figure 3.9 Low temperature dependence of the resistance for low-stage fibrous acceptor GICs, with various hosts and intercalates, showing the logarithmic increase in resistivity with decreasing temperature, charateristic of localization and electron–electron interaction effects. All data are normalized to the minimum value of the resistance (Piraux, 1990).

In low stage acceptor graphite fiber intercalation compounds high resolution low temperature resistivity measurements performed by Piraux and co-workers (1985) displayed logarithmic increases of the resistivity with decreasing temperature for different host structures and intercalates. In most cases, 0.1% to 1% increases in electrical resistivities were detected over a decade of temperature in the liquid helium range (Fig. 3.9). Except for the case of fluorine intercalation compounds, the increase in resistivity was thus found to be usually small above 1.5 K, the lowest temperature at which measurements were performed. The better the samples are, the smaller is the increase in resistance due to localization (Piraux, 1990). This increase in zero-field resistivity is accompanied by a negative magnetoresistance.

The most spectacular effects of the localization and Coulomb interaction effects were observed on fiber-based compounds of low crystalline perfection. This is the case for fluorine compounds where intercalation may lead to significant distortion of the graphene layers.

Weak localization effects have been observed in the electrical resistivity of all intercalated carbon fibers of low structural perfection, whether PDFs or VGCFs. The compounds investigated were found to verify the weak disorder condition $k_F l \gg 1$. The temperature dependence of the resistivity increase was found consistent with the 2D electronic structure and the results obtained concerning the temperature and magnetic field dependences of the effect were found to fit the theoretical predictions (Piraux, 1990).

Finally, for comparison, we present in Fig. 3.10 the effect of intercalation by donor (Fig. 3.10a) and acceptor (Fig. 3.10b) species on the temperature dependence of the resistivity of SWNT samples. In both cases, we observe, as for the case of bulk fibers, a decrease of resistivity after intercalation (Lee *et al*., 1997).

6.3 The limits of electrical conductivity

Earlier work on the electrical resistivity of graphite intercalation compounds was stimulated by the promise of realizing electrical conductors with conductivities that could reach or even exceed that of copper. A question which might be raised now is to what extent one could increase the electrical conductivity of GICs. We now know the answer for the particular case metallic chlorides GICs (Issi, 1992).

In the 2D model derived for acceptor compounds (Blinowski *et al*., 1980), the carrier density, N, varies as k_F^2 and the effective mass, m*, varies linearly with k_F, the Fermi wave vector. Thus, we may express the 2D electrical conductivity:

$$\sigma_{2D} \sim k_F \cdot \tau(k_F) \tag{5}$$

and since the relaxation time, $\tau(k_F)$, should decrease with increasing wave number or carrier density:

$$\tau(k_F) \sim k_F^{-a} \tag{6}$$

One may see from relations (5) and (6) that, if a is larger than 1, the electrical conductivity decreases when the k_F or N increases. Since at room temperature one should expect a value of a equal or higher than 1, the conductivity should either remain constant or decrease when the charge transfer increases, provided we remain in the range where the dispersion relation is linear in k. If scattering by in-plane graphitic phonons is the dominant mechanism, $a = 1$ (Pietronero and Strässler, 1981), then $\tau(k_F) \sim k_F^{-1}$, and in this case one should expect a conductivity independent of charge transfer.

So, at least for metallic chloride GICs, the resistivity could hardly be less than roughly $5 \times 10^{-6} \Omega\,\text{cm}$, the value of the intrinsic resistivity at this temperature. However, one should add to this intrinsic resistivity that of the residual resistivity. Since the latter is governed by lattice defects and there are defects inherent to the intercalation process, the resistivities of metallic chloride GICs should in practice be higher than $5 \times 10^{-6} \Omega\,\text{cm}$.

6.4 Thermal conductivity

We have already pointed out in Section 4 the mechanisms which contribute to the thermal conductivity of solids and discussed the case of pristine carbons and graphites. Let us consider now how intercalation is expected to modify the thermal conductivity of pristine fibers.

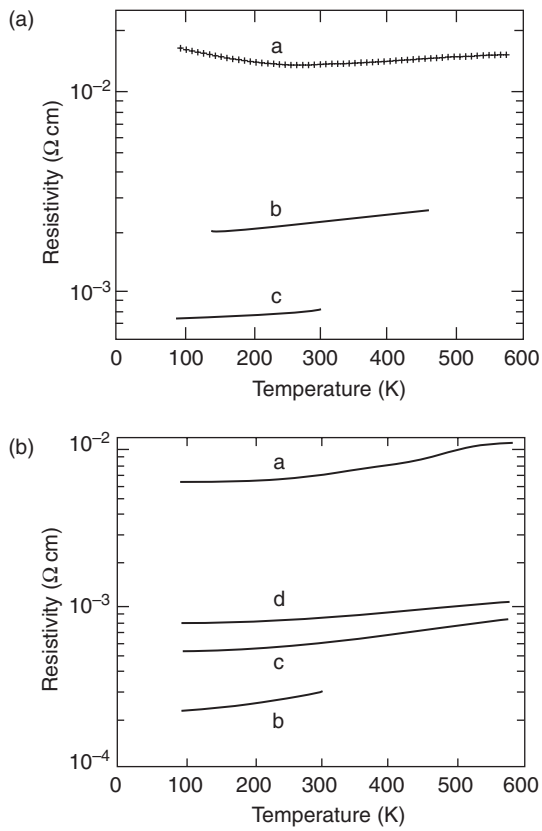

Figure 3.10 (a) The effect of potassium intercalation on the temperature dependence of the resistivity of a bulk SWNT sample. Curve a, pristine material from a different batch than in Fig. 3.6; curve b, after doping with potassium; curve c, after heating in the cryostat vacuum to 580 K overnight; curve d, after 3 days at 580 K (Lee *et al*., 1997). (b) The effect of Br_2 intercalation on the temperature dependence of the resistivity of a bulk SWNT sample. Curve a, pristine material; curve b, saturation doped with Br_2; curve c, after heating in the cryostat vacuum to 450 K for several hours (Lee *et al*., 1997).

On one hand, according to the Wiedemann–Franz relation, which relates the electronic thermal conductivity, κ_E, to the electrical conductivity, σ:

$$\kappa_E = L\,T\,\sigma \tag{7}$$

one should expect an increase in the electronic thermal conductivity in intercalation compounds. On the other hand, because of lattice defects introduced by intercalation, the lattice thermal conductivity should decrease. This is what is observed. The net result of intercalation is a decrease of the total thermal conductivity at high temperature and an increase at low temperature with respect to that of the pristine material (Fig. 3.11) (Issi, 1992). Here also, as is the case for the pristine material (cfr. Section 4), from the low temperature lattice thermal conductivity, one may estimate the size of the large scale defects and the concentration of point defects.

It is worth noting that when the electrical conductivity and electronic thermal conductivity may both be expressed in terms of the same relaxation time, the Lorenz ratio, L, takes the value of the Lorenz number ($L_o = 2.44 \times 10^{-8} V^2 K^{-2}$). This holds for a degenerate free electron system which undergoes elastic collisions. Thus $L = L_o$ for metals in the temperature ranges where this last conditions apply. This is the case in the low temperature residual resistivity range when scattering is dominated by impurities and lattice defects. The Wiedemann–Franz law holds also around and above the Debye temperature when large angle intravalley electron–acoustic phonon interaction is the main scattering mechanism.

In Fig. 3.11 we present on a log-log plot the temperature dependence of the thermal conductivity of a benzene-derived carbon fiber (BDF) intercalated with $CuCl_2$ (Piraux *et al.*, 1986). For comparison we have presented on the same figure the temperature dependence of the thermal conductivity of the pristine material heat treated at the same temperature

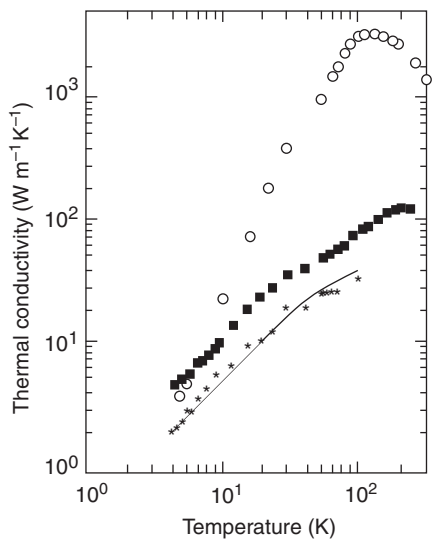

Figure 3.11 Temperature dependence of the thermal conductivity of $CuCl_2$ intercalated benzene-derived carbon fibers compared to that of pristine fibers (open circles) heat treated at the same temperature (3,000 °C). The total measured thermal conductivity of the intercalated sample (black squares) is separated into its electronic (curve) and lattice (crosses) contributions (Piraux *et al.*, 1986).

(3,000 °C). Starting from the liquid helium temperature range, the thermal conductivity increases with increasing temperature up to nearly 230 K. Using the Wiedemann–Franz relation, the total measured thermal conductivity was separated into its electronic and lattice contributions (cfr. Section 6.5).

It may be seen in Fig. 3.11 that, in contrast to the pristine material, electronic conduction in GICs may contribute to heat transport well above the liquid helium temperature range. This is due to the large increase in the charge carrier concentration in GICs resulting from charge transfer and is more pronounced at low temperatures where the lattice thermal conductivity of the pristine material decreases almost quadratically with temperature.

It is worth adding that, contrary to the case of intercalated HOPG, where the thermal conductivity of both acceptor and donor compounds have been investigated, for intercalated fibers, only a few acceptor compounds have been studied. The results obtained with HOPG and fibers as hosts were found to be qualitatively the same.

6.5 Separation of the electronic and lattice contributions

Contrary to the case of pristine fibers where the thermal conductivity is generally dominated by the lattice contribution above the liquid helium temperature range, in GICs an electronic contribution may be important at any temperature. In that case, in order to interpret the results it is necessary to be able to separate the two contributions. One of the great advantages of measuring the thermal conductivity on intercalated fibers is that, contrary to bulk graphites this separation can be done. For that purpose, one has to measure on the same sample the electrical and thermal conductivities. In fibers, this resistivity can be measured by means of a DC method (cfr. Section 2). Then, introducing the values obtained in the Wiedemann-Franz relation (relation 7), one may readily calculate the corresponding electronic thermal conductivity at a given temperature. By subtracting the latter from the total measured thermal conductivity (relation 2), one obtains the lattice contribution. This method is applicable in the temperature range where the Wiedemann–Franz ratio is equal to L_o, the free electron Lorentz number.

Generally, intercalated fiber exhibit high residual resistivities which may dominate the total resistivity up to relatively high temperatures (Issi and Nysten, 1998). In that case the Wiedemann–Franz law is expected to be valid over a wide temperature range. This is particularly true for pitch-derived fibers of poor structural perfection, where the electrical resistivity is very weakly temperature dependent (Issi and Nysten, 1998). In that case the electronic thermal conductivity can be directly computed over a large temperature range from the measured electrical resistivity via the Wiedemann–Franz law using the free electron Lorentz number (Piraux *et al*., 1985, 1986).

So, the fibers present two major advantages with respect to HOPG when we need to separate the two contributions to the thermal conductivity. First, one can measure electrical and thermal conductivities on the same sample, and second the Wiedemann–Franz law applies over much wider temperature ranges. The result of such a separation for a $CuCl_2$ fibrous compound is presented in Fig. 3.11.

6.6 Thermoelectric power

In Fig. 3.12 we present the temperature dependence of the thermoelectric power of the BDF intercalated with $CuCl_2$ (Piraux *et al*., 1986), which thermal conductivity is presented

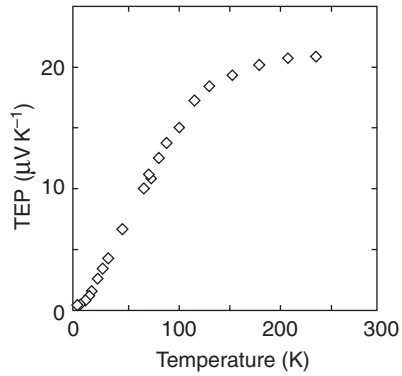

Figure 3.12 Temperature dependence of the thermoelectric power of $CuCl_2$ intercalated benzene-derived carbon fibers, which thermal conductivity is presented in Fig. 3.11 (Piraux *et al*., 1986).

in Fig. 3.11 and discussed in Section 6.4. The thermoelectric power is positive over the entire temperature range, indicating that hole conduction dominates. The temperature dependence is typical of that of all low-stage GICs whether fibrous or bulk. It starts with a linear dependence in the lowest temperature range, then increases more rapidly and finally tends to saturate around 200 K.

From the low temperature linear temperature dependence of the thermoelectric power of stage-2 compounds at low temperatures, Piraux and co-workers (1988) were able to estimate the Fermi energies of a few compounds.

Also, a thorough analysis of the data obtained on the thermoelectric power of various acceptor intercalation compounds lead to the conclusion that there is a dominant phonon drag contribution for low stage acceptor GICs in the high temperature range (Issi, 1992). This is a unique situation which should be attributed to the particular 2D nature of acceptor GICs.

7 Sample characterization

We have recently shown (Issi and Nysten, 1998) how the residual resistivity and the magnetoresistance, provide information about the lattice defects, while the interpretation of the temperature variation of the ideal electrical resistivity shed some light on electron–phonon and electron–electron interactions. We have also seen that thermal conductivity measurements were a useful source of information about lattice defects.

One may characterize and determine the defect structure of various types of carbon fibers, whether pristine or intercalated. This approach usefully complements the information obtained by means of more powerful techniques which probe the material at the microscopic level, such as SEM, high resolution TEM, X-ray diffraction, STM, AFM, … Contrary to these microscopic techniques, which are very localized and thus only probe a very tiny portion of the sample, electrical and thermal transport data give an overall view over the entire macroscopic sample. In addition, in some cases transport data are sensitive to defects which could not be detected by other techniques.

As was seen above, *thermal conductivity* measurements performed in the liquid nitrogen temperature provide a direct way to determine the in-plane coherence length in pristine fibers. This is also true for the intercalation compounds. Thus, from comparative measurements on pristine and intercalated samples, one is in a position to appreciate how the intercalation process affects the in-plane coherence length. *Electrical resistivity* measurements, though they are extremely sensitive to defects revealing very large differences in residual resistivies for samples with different defect structures, are more delicate to analyze in detail in the case of pristine fibers. In principle, *magnetoresistance* measurements probe the mobilities, thus are essentially sensitive to the scattering mechanism. The *thermoelectric power* is very sensitive to the carrier densities, and although it depends on the nature of the scattering mechanism, it is not affected by its intensity. As it is the case for the electrical resistivity, the thermoelectric power data are delicate to interpret in pristine carbons and graphites.

8 Carbon fiber composites

8.1 Introduction

One may look at *Polymer–matrix composites* filled with carbon fibers in two ways. The first approach consists in considering the exceptional mechanical properties or thermal conductivity of carbon fibers associated to their specific geometry and decide to use these properties in order to realize a practical device. Since the tiny and breakable fibers are usually delicate to handle, the solution is to embed them in a matrix which will distribute the mechanical stresses and connect the fibers to the macroworld via the matrix. One may then use the composite wherever lightweight mechanical structures or efficient bulk thermal conductors are needed.

Alternatively, one may think of improving the electrical or thermal properties of polymeric materials, which are generally electrical insulators and poor thermal conductors, by realizing polymer matrix composites filled with conductive fibers.

From the previous sections it was obvious that it is possible to tailor carbon fibers at the microstructural level to obtain specific electrical or thermal conductivities, since these properties are very sensitive to the in-plane coherence length. This was found to be particularly interesting for the case of the thermal conductivity. Indeed, by choosing adequately the precusor and by increasing the heat treatment temperature higher thermal conductivities are obtained. We were tailoring in fact the conductivity at the *microscopic level*. In a similar way, composites allow to tailor the properties of a given material at a *macroscopic level*. By this way, one is able to realize efficient heat transfer devices and in some cases heat hyperconductors, with the highest thermal conductivities which could be attained in a practical material.

8.2 Electrical conductivity

Polymer–matrix composites filled with a high enough percentage of carbon fibers may be *electrically conductive*. To attain this goal, the percentage of fibers should exceed the percolation threshold, which is relatively low for these fillers because of their high aspect ratio, i.e. their high length to cross section ratio. A transition from insulating to electrically conductive behavior occurs at the percolation threshold (see e.g. Carmona, 1988).

The typical dependence of the electrical resistivity of the composite on the fiber volume fraction is as follows (Carmona, 1988; Demain, 1994). For low concentrations, the dilute concentration regime, the fibers are randomly distributed in the matrix forming small aggregates or single inclusions which are separated by the polymer matrix. Since the latter has a very high electrical resistivity, the electrical resistivity of the composite is very high. An increase in the fiber concentration leads to an increase of the number and size of the aggregates. Eventually, some growing aggregates get in contact with their nearest neighbors and merge into larger clusters. For larger concentrations, an "infinite" cluster is formed. Around this concentration, i.e. at the percolation threshold, the electrical resistivity of the composite dramatically drops by 10–15 orders of magnitude. This results from the creation of a continuous path of electrically conductive fibers across the entire sample.

With further increase of the fiber concentration, new electrically conductive paths may be created inside the infinite cluster or may link to this cluster aggregates which were previously isolated. This leads to a monotonic decrease of the composite electrical resistivity with further increase in fiber content.

8.3 Thermal conductivity

The need for high thermal conductivity materials is increasingly recognized nowadays for technical applications. This is true when we need to improve heat exchanges in practical devices or during a manufacturing process. In that context polymeric matrix composites present the great advantage of having very low specific gravity as compared to metals and their alloys. This is particularly interesting for applications in space and airborne systems. To this advantage, one must add their relatively high chemical resistance, their ease of processing and energy saving.

For unidirectional composites with highly conductive continuous pitch-based carbon fibers, room temperature thermal conductivities comparable to that of pure copper are now readily attained (Nysten and Issi, 1990). With chopped fibers, thermal conductivities superior to that of metallic alloys may be obtained in composites, as will be seen below. Thus, with carbon fibers one may tailor at the macroscopic scale the thermal conductivity of composites to the desired values for practical applications.

For the case of composites containing aligned highly conducting *continuous carbon fibers* the result of fiber addition on the total thermal conductivity of the composite is straightforward. It was shown experimentally in that case that the thermal conductivity of the composite along the fiber axis direction obeys the simple law of mixtures. Since the thermal conductivity of the polymer is generally negligible with respect to that of the fiber, this means that it is equal to the product of the fiber volume fraction and thermal conductivity. In order to check that, the thermal conductivity of the fibers were first determined and the result was compared with those obtained for the composite as a function of fiber volume fraction (Nysten and Issi, 1990). With the composites investigated, thermal conductivities higher than that of pure copper were obtained. This result is obvious when we consider that pitch-derived carbon fibers with thermal conductivities exceeding $1{,}000\,\mathrm{Wm^{-1}K^{-1}}$ are now available.

The case of composites with *chopped fibers* is far more complicated to deal with. In that case, though there is a relation between the thermal conductivity of the fiber and that of the composite, this relation is not staightforward as for the case of unidirectional composites with continuous fibers. In addition to the volume fraction and fiber conductivity, there is

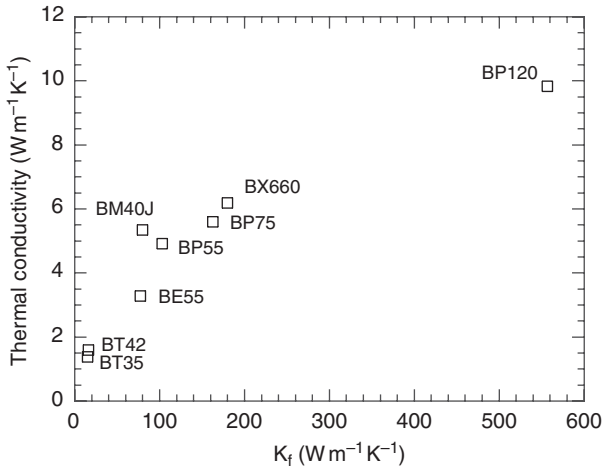

Figure 3.13 Room temperature thermal conductivity of chopped fiber-polycarbonate matrix composites versus the thermal conductivity of the fibers (Demain, 1994) for a given volume fraction. For each experimental point the corresponding type of fiber is indicated.

a large variety of parameters to control in order to improve the thermal conductivity of the composite (Demain, 1994): fiber length, length to diameter ratio, average orientation of the fibers in the composite, the fiber-matrix interface, …

As an example, we present in Fig. 3.13 the room temperature thermal conductivity of chopped fiber-polycarbonate matrix composites versus the thermal conductivity of the fibers (Demain, 1994), all other parameters being almost the same. We may see that for carbon fibers with a thermal conductivity of 550 $Wm^{-1}K^{-1}$, one may elaborate a composite with a thermal conductivity of ~10 $Wm^{-1}K^{-1}$, which compares fairly well with that of metallic alloys. Figure 3.14 shows the relation at 300 K between the thermal conductivity of a chopped fiber–polycarbonate matrix composite versus fiber volume fraction for fibers of different lengths. The heat flow is parallel to the plane of the composite which is in the form of a plate.

We have seen above that for the case of electrical conductivity (Section 8.2), the transition from electrically insulating to electrically conductive state, which is explained in the frame of the percolation theory, is abrupt. However, such a rapid transition does not occur in the case of thermal conductivity. The reason for that is that the mechanisms responsible for electrical and thermal conduction are different. Electrical conductivity is always generated by charge transport, while the thermal conductivity of the fibers at room temperature and of the polymeric matrix is due exclusively to phonons. Besides, while the polymeric matrix is an electrical insulator and thus cannot carry electrical current, it may still conduct heat to some extent and thus may still transfer some heat from one fiber to the other.

Thus the dependence of the composite thermal conductivity on the fiber concentration (Fig. 3.14) is expected to be different from that of the electrical conductivity discussed above (Section 8.2). We may tentatively explain this behavior as follows (Demain, 1994). Within the aggregates of fibers, the conductance of the polymer separating the fibers which are very close to them is of the same order of magnitude as that of the fibers, yielding thus highly

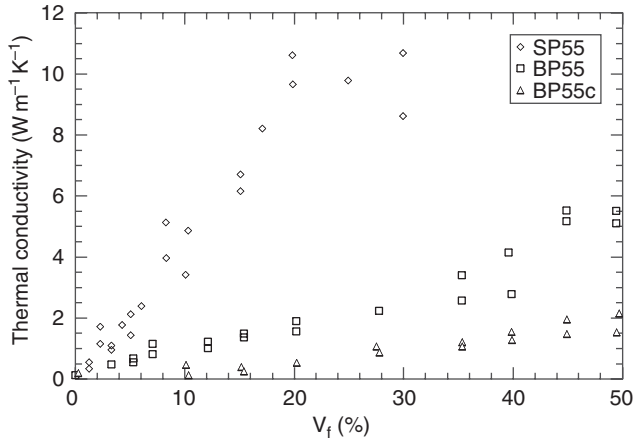

Figure 3.14 Room temperature dependence of the thermal conductivity of a chopped fiber (P55)-polycarbonate matrix composite versus fiber volume fraction (Demain, 1994). The heat flow is parallel to the plane of the composite in the form of a plate. The different sets of experimental points are relative to composites with fibers of different average lengths: roughly 40 gm for BP55c, 100 gm for BP55, and 360 gm for SP55. From this figure one may also appreciate the effect of fiber length on the conductivity for a given volume fraction.

thermally conductive regions inside the composite. At low fiber concentrations, those aggregates are separated from each other by resin rich regions which are less conductive and thus reduce the heat transfer across the sample.

One may consider the polymer loaded with particles whose sizes and geometries are those of the aggregates and whose thermal conductivity is intermediate between that of the polymer and the filler. When the concentration is increased, the average distances between the aggregates decreases thus increasing the conductance of the polymer separating them and hence increasing the thermal conductivity of the composite. Finally, when the fiber concentration exceeds the percolation threshold, an infinite aggregate is formed. In the absence of resin rich regions between the aggregates, the conductance of the polymer close to the fibers dominates the composite thermal conductivity. Any further increase of the fiber concentration increases the number of paths for the heat and areas for heat transfer from one fiber to another.

Hence, the transition from a concentration range where the thermal conductivity of the composite is depending on the conductance of the polymer between aggregates to a concentration range where the conductance within the aggregates dominates, could explain the change from a linear to a non linear $K_c(V_f)$. This interpretation is corroborated by results of electrical resistivity measurements which were used to probe the type of arrays formed by the fibers in the matrix.

When we compare the results relative to *in-plane* and *out-of-plane* thermal conductivities (Demain, 1994), we observe that for the same fiber volume fraction, in-plane thermal conductivities are always much larger than out-of-plane thermal conductivities. Also, both in-plane and out-of-plane conductivities increase linearly with fiber concentrations in the range 0–30%, whereas they generally increase more rapidly for larger concentrations.

Concerning the effect of the *average fiber length* for concentration ranging from 0% to 30%, it was shown that thermal conductivities comparable to that of a composite filled with continuous random in-plane fibers could be attained with samples whose average fiber lengths are around 500 μm.

It is interesting to note that as for the case of fibers, transport measurements may be used to characterize to some extent composites. For example, electrical resistivity and magnetoresistance measurements may be used to gain information on the fiber orientation and the way the fibers are dispersed in the matrix (Demain, 1994).

9 Conclusions

In this chapter our aim was to outline the specific aspects of transport in carbon fibers with respect to bulk carbons and graphites in particular, but also, more generally with respect to other solids. We have considered carbon nanotubes as one variety of fibers, but have refrained in discussing in detail their properties, since they are the object of other chapters in this series.

We have shown that, in addition to practical aspects, the various structures of carbon fibers and their particular geometry have lead to interesting observations, which could not be made on bulk carbons and graphites. This is the case for high resolution electrical resistivity measurements which lead to the discovery of quantum transport effects on carbons and graphites. We have also shown that it was possible to separate the electronic and lattice contributions to the thermal conductivity in intercalated fibrous compounds

Leaning heavily on the basic concepts which we have discussed in I, we have mainly concentrated in this chapter on the specific aspects related to fibers which were not already discussed in detail in I. Emphasis was thus placed on the thermal conductivity of pristine fibers, the effect of intercalation on the transport properties, and the electrical and thermal conductivities of composites. Besides, we have discussed in brief the experimental difficulties associated to measurements on fibrous materials.

Note added in proof

Since this chapter was written the thermal conductivity and thermoelectric power of individual multiwalled carbon nanotubes has been measured (Kim *et al*., Phys. Rev. Letters, 87 (2001)). As expected, the room temperature thermal conductivity was found to exhibit very high values ($3000\,\mathrm{Wm^{-1}K^{-1}}$).

References

Allen, G. and Issi, J.-P. (1985) *Proceedings of ECCM-1*, 447.

Bayot, V., Piraux, L., Michenaud, J.-P., and Issi, J.-P. (1989) Phys Rev. **B40**, 3514.

Blinowski, J. and Rigaux, C. (1980) Synth. Metals **2**, 277.

Bright, A. A. (1979) Phys. Rev. **B20**, 5142.

Bright, A. A. and Singer, L. S. (1979) Carbon **17**, 59.

Carmona, F. (1988) Ann. Chim. Fr. **13**, 395–443.

Chieu, T. C., Dresselhaus, M. S., and Endo, M. (1982) Phys. Rev. **B26**, 5869.

Chieu, T. C., Dresselhaus, M. S., Endo, M., and Moore, M. A. W. (1983) Phys. Rev. **B27**, 3686.

Demain, A. (1994) *Thermal conductivity of polymer-chopped carbon fiber composites*, PhD thesis, Université Catholique de Louvain, Louvain-la-Neuve.

Dresselhaus, M. S. and Dresselhaus, G. (1981) Adv. Phys. **30**, 139.

Dresselhaus, M. S., Dresselhaus, G., Sugihara, K., Spain, I. L., and Goldberg, H. A. (1988) *Graphite Fibers and Filaments*, Springer Series in Materials Science 5, Springer-Verlag.
Endo, M., Tamagawa, I., and Koyama, T. (1977) Jpn. J. Appl. Phys. **16**, 1771.
Endo, M., Hishiyama, Y., and Koyama, T. (1982) J. Phys. D: Appl. Phys. **15**, 353.
Gallego, N. C., Eddie, D. D., Nysten, B., Issi, J-P., Treleaven, J. W., and Deshpande, G. V. (2000) Carbon **38**, 1003–1010.
Hone, J., Ellwood, I., Muno, M., Mizel, A., Cohen, M. L., Zettl, A., Rinzler, A. G., and Smalley, R. E. (1998) Phys. Rev. Letters **80**, 1042.
Issi, J.-P. Heremans, J., and Dresselhaus, M. S. (1983) Phys. Rev. **B27**, 1333.
Issi, J.-P. and Piraux, L. (1986) Annales de Physique, **11**(2), 165.
Issi, J.-P. (1992) "Transport properies of metal chloride acceptor graphite intercalation compounds," in Zabel, H. and Solin, S. A. eds, *Graphite Intercalation Compounds II*, Springer Series in Materials Science, Vol. 18 (Springer-Verlag, Berlin).
Issi, J.-P. and Nysten, B. (1998) "Electrical and thermal transport properties in carbon fibers," in Donnet, J.-B., Rebouillat, S., Wang, T. K., and Peng, J. C. M. eds *Carbon Fibers*, New-York Marcel Dekker, Inc.
Issi, J.-P. and Charlier, J.-C. (1999) "Electrical transport properties in carbon nanotubes," in *Science and Technology of Carbon Nanotubes*, Tanaka, K. ed., Elsevier, London.
Issi, J.-P. (2000) "Electronic Conduction" in Delhaes, P. ed. (1964) *World of Carbon*, Gordon and Breach, UK.
Klein, C. A. (1964) J. Appl. Phys. **35**, 2947.
Langer, L., Stockman, L., Heremans, J. P., Bayot, V., Olk, C. H., Van Haesendonck, C., Bruynseraede, Y. and Issi, J.-P. (1994) *J. Mater. Res.* **9**, 927–932.
Langer, L., Bayot, V., Grivei, E., Issi, J.-P., Heremans, J. P., Olk, C. H., Stockman, L., Van Haesendonck, C. and Bruynseraede, Y. (1996) Phys. Rev. Letters **76**, 479.
Lee, R. S., Kim, H. J., Fischer, J. E., Thess, A., and Smalley, R. E. (1997) Nature, **388**, 255.
Mrozowski, S. and Chaberski, A. (1956) Phys. Rev. **104**, 74.
Nysten, B., Piraux, L., and Issi, J.-P. (1987) in D. W. Yarbrough, ed. *Thermal Conductivity* **19**, Plenum Press, New York, 341.
Nysten, B. and Issi, J.-P. (1990) Composites **21**, 339.
Nysten, B., Issi, J.-P., Barton, R., Jr. Boyington, D. R., and Lavin, J. G. (1991a) J. Phys. D: Appl Phys, **24**, 714.
Nysten, B., Issi, J.-P., Barton Jr., R., Boyington, D. R., and Lavin, J. G. (1991b) Phys. Rev. **B44**, 2142.
Pietronero, L. and Strässler, S. (1981) Synthetic. Metals **3**, 213.
Piraux, L., Nysten, B., Issi, J. P., Salamanca-Riba, L., and Dresselhaus, M. S. (1986) Solid State Commun. **58**, 265.
Piraux, L., Nysten, B., Haquenne, A., Issi, J.-P., Dresselhaus, M. S., and Endo, M. (1984) Solid State Commun. **50**, 69.
Piraux, L., Issi, J.-P., Michenaud, J.-P., McRae, E., and Marêché, J. F. (1985) Solid State Commun. **56**, 567.
Piraux, L., Bayot, V., Michenaud, J.-P., Issi, J.-P., Marêché, J. F., and McRae, E. (1986a) Solid State Commun. **59**, 711.
Piraux, L., Issi, J.-P., Salamanca-Riba, L., and Dresselhaus, M. S. (1986b) Synthetic Metals, **16**, 93.
Piraux, L., Issi, J. P., and Coopmans, P. (1987) Measurement, **5**, 2.
Piraux, L. (1990) Mater. J. Res. **5**, 1285.
Robson, D., Assabghy, F. Y. I., and Ingram, D. J. E. (1972) J. Phys. D: Appl. Phys. **5**, 169.
Robson, D., Assabghy, F. Y. I., Cooper, E. G., and Ingram, D. J. E., J. Phys. D: Appl. Phys.